RESEARCH PAPER

Unlocking the potential of PLGA/thymoquinone nanoparticles: a promising frontier in asthma therapeutics

Mohsen Rahmanian[1#], Samereh Ghazanfary[2#], Mehran Vatanchian[3], Ali Haghbin[4], Fatemeh Oroojalian[5,2*]*

[1] *School of Medicine, North Khorasan University of Medical Sciences, Bojnurd, Iran*
[2] *Department of Medical Nanotechnology, School of Medicine, North Khorasan University of Medical Sciences, Bojnurd, Iran*
[3] *Department of Anatomical Sciences and Pathology, School of Medicine, North Khorasan University of Medical Sciences, Bojnurd, Iran.*
[4] *Department of Pediatrics, School of Medicine, North Khorasan University of Medical Sciences, Bojnurd, Iran*
[5] *Natural Products and Medicinal Plants Research Center, North Khorasan University of Medical Sciences, Bojnurd, Iran*

 # Equally first authors
**Equally corresponding authors*

ABSTRACT

Objective(s): To formulate mPEG-PLGA/Thymoquinone nanoparticles for enhanced biological uptake and therapeutic effectiveness of thymoquinone in asthmatic mice induced with ovalbumin (OVA) administration.

Materials and Methods: mPEG-PLGA/thymoquinone nanoparticles generated using nanoprecipitation were studied for size distribution (dynamic light scattering), in vitro release profile, drug entrapment efficiency (EE), and appearance (scanning electron microscopy). Cytotoxicity assessment via the MTT assay using L929 and RAW 264.7, (a mouse macrophagic cell line) confirmed that the formulation was biocompatible at concentrations up to 1000 µg/m. Drug release was analyzed at 37°C and 25°C over 8 days. In vivo efficacy was evaluated in mice with OVA-induced asthma, measuring OVA-specific IgE and cytokine levels (IL-4, IL-13), and lung histopathology (H&E staining).

Results:The nanoparticles exhibited an average size of 255 nm and EE of 68.16%. In vitro release showed early rapid discharge with a subsequent gradual course. In vivo, mPEG-PLGA/Thymoquinone significantly reduced serum OVA-specific IgE levels and Th2-type cytokines (IL-13 and IL-4) in bronchoalveolar lavage fluid (BALF) compared to PBS and thymoquinone treatments. Histopathological analysis (H&E staining) confirmed that mPEG-PLGA/Thymoquinone significantly reduced perivascular and peribronchial inflammation, edema, and epithelial thickness, demonstrating superior efficacy compared to Dexamethasone and free Thymoquinone in some parameters.

Conclusion: mPEG-PLGA/Thymoquinone nanoparticles provide an effective strategy for enhancing thymoquinone's therapeutic potential in asthma by improving drug delivery, reducing inflammation, and modulating the immune response.

Keywords: *Asthma, Nanoparticles, Thymoquinone, Bronchoalveolar lavage, Therapeutics.*

How to cite this article

Rahmanian M, Ghazanfary S, Vatanchian M, Haghbin A, Oroojalian F. Unlocking the potential of PLGA/thymoquinone nanoparticles: a promising frontier in asthma therapeutics. Nanomed J. 2025; 12: 1-. DOI: 10.22038/NMJ.2025.86007.2155

INTRODUCTION

Asthma is associated with persistent inflammation of the pulmonary system and affects approximately 300 million individuals around the globe, with projections indicating beyond 100 million new cases by 2025 (1). The economic burden of asthma is substantial, with average annual costs estimated at $1,900 per patient in Europe and $3,100 in the United States (2). Allergic asthma is characterized by elevated serum levels of Th2-derived cytokines, notably IL-4 and IL-13, which contribute to bronchial hyperreactivity and accumulation of immune cells into the pulmonary parenchyma. This condition also involves the proliferation of goblet cells and smooth muscle, accompanied by increased serum IgE levels (3, 4). Additionally, cytokines IL-9, IL-13, and IL-1 are integral to asthma pathology. IL-9, a Th2 cytokine, plays a significant role in bronchial hyperreactivity, abnormal sputum accumulation, and morphological alterations within the respiratory tract (5, 6). Bronchial hyperresponsiveness is a fundamental feature of asthma, resulting in airway constriction and associated symptoms. Assessing this phenomenon is crucial for evaluating the effectiveness of asthma management strategies, typically performed through bronchial challenge tests(7). Airway remodeling in asthma

*Corresponding author(s) Email:
dr.haghbin@gmail.com,oroojalian.f@gmail.com.
Note. This manuscript was submitted on February 10, 2025; approved on July 03, 2025.

encompasses various structural modifications, including subepithelial fibrosis, increased smooth muscle mass, and epithelial alterations, collectively contributing to airway narrowing, mucous hypersecretion, and suboptimal clinical outcomes (8).

The Global Initiative for Asthma (GINA) emboldens anti-inflammatory and bronchodilator therapies, with a focus on severity classification and a step-wise approach to treatment (9). Inhaled corticosteroids (ICS) are particularly highlighted, with formoterol recommended as a reliever in mild asthma, as well as in severe disease where it is regarded as part of maintenance-and-reliever therapy (10).

The management of severe asthma presents considerable challenges due to the limited efficacy of current therapeutic options. This is compounded by the need for a systematic, control-oriented approach, which is often hindered by imprecise assessment tools and poor adherence rates (9). Patients with refractory severe asthma face even fewer treatment options, with primary recommendations centered around oral glucocorticoids and anti-IgE antibody therapy (11).

Although corticosteroids are effective in controlling asthma, their lack of specificity can lead to side effects and adherence difficulties, particularly in pediatric and adolescent populations (12, 13). Consequently, targeted therapies, such as humanized monoclonal antibodies targeting IgE ILs-13, 4, and 5, TNF, and IL-13, have been placed in the center of attention. While anti-IgE antibodies are used as a remedy for allergic diseases, thei r adverse effects are noticeable, including local reactions like pain, bruising, swelling, and erythema, as well as systemic reactions such as persistent headache, impaired kidney function, vascular embolic events, and hemolytic incidents (14, 15). Hence, there is a pressing need to develop more effective and precisely targeted therapies tailored to severe asthma.

Research has demonstrated that natural products like medicinal plants may offer significant benefits in different diseases (16) like asthma treatment, owing to their potential reduced side effects and efficacy comparable to conventional pharmacological interventions (17). In parallel, nanomedicine presents a novel discipline through which current therapies can experience extensive surge in efficiency and safety. Of particular note, nanoparticle application for targeted drug delivery to airway epithelial cells holds substantial potential in alleviating or reversing airway dysfunction associated with asthma (18).

In recent years, nanotechnology has become a groundbreaking method in medicine, providing novel strategies for both the diagnosis (nanosensors) (19-22) and treatment (drug and gene delivery) (23-26) of the diseases. Polymeric nanoparticles, especially those formulated from PLGA-PEG, have received FDA approval and confer multiple advantages. These nanoparticles can enhance the effectiveness of existing medications, enable sustained drug release, minimize drug-induced side effects, and improve therapeutic outcomes (27, 28). Additionally, preclinical studies suggest that PLGA-PEG nanoparticles exhibit protective mechanisms against airway complications and demonstrate an ability to evade mucus obstruction (29).

Thymoquinone ($C_{10}H_{12}O_2$), the principal bioactive compound derived from Nigella sativa, has been extensively researched and identified as exhibiting therapeutic features, comprising beneficial effects against inflammation, neoplasms, hypertension, depression, and pathogenic microorganisms (30, 31). It has also been employed to fight against diabetes, rheumatoid arthritis, hypertension, and hypercholesterolemia (30). In the context of asthma research, Thymoquinone has been particularly noted for its ability to curb inflammatory and oxidant processes. It has been shown to suppress T helper 2 (Th2) cytokines while inhibiting the inflammatory effects mediated by lipoxygenase (LO) and cyclooxygenase (COX) (32, 33). Moreover, Thymoquinone has demonstrated promise in the treatment of various inflammatory respiratory conditions, with studies indicating its ability to reduce leukotriene B4 and C4 levels, lung tissue eosinophilia, and goblet cell hyperplasia (34, 35). Accordingly, our study aimed to enhance the solubility, stability, and transport of thymoquinone across biological barriers, while simultaneously improving its protection against degradation and therapeutic efficacy. To achieve these objectives, thymoquinone was encapsulated within PLGA-PEG nanoparticles. We subsequently investigated if mPEG-PLGA/Thymoquinone formulations could mitigate asthma-associated inflammation.

MATERIAL AND METHODS

Materials

PEG-PLGA and thymoquinone were obtained from Sigma-Aldrich (Germany). Other chemicals used included phosphate-buffered saline (PBS), 3-(4,5-dimethylthiazol-2-yl)-2,5-diphenyltetrazolium bromide (MTT), Polysorbate-80, and Dulbecco's modified Eagle's medium (DMEM) attained from Sigma-Aldrich (Germany). ELISA kits purchased

from Karmania Pars Gene (Iran) were used to assess cytokine levels. Analytical grade chemicals were used in all experiments.

Animals

56-day-aged BALB/c female mice were obtained from Iran's Pasteur Institute (Karaj, Iran). The mice were housed in standardized environmental and nutritional conditions throughout the experimental period. The investigation received clearance from the ethical board of the affiliated institution and all experimental methods followed the ethical standards for animal research set by the Research Ethics Committee.

Nanoparticle preparation

In our investigation, we employed the nanoprecipitation method for synthesizing nanoparticles. In the first step, the aqueous phase, comprising surfactant (polyvinyl alcohol, PVA, 0.1%-0.3% w/v) and stabilizer (Polysorbate-80, 1 ml), is prepared. The organic phase contained PLGA (50:50, MW ~50 kDa) and thymoquinone (20 mg), dissolved in oleic acid (1 ml) and stabilized with lecithin (0.1-0.4%) (36).

In a dropwise manner, the organic phase was added to the aqueous phase and subjected to intense stirring at room temperature for 24 hours. Furthermore, Nanocapsules loaded with thymoquinone were attained. The resultant dried nanoparticles were stored until further experimentation was needed.

Histopathological examination

Out of 10 mice in each group (a total of nine groups), five were chosen for histological evaluation. Lung tissues were excised, cleaned with PBS, and immersed in 10% formalin for fixation. Each preserved tissue was encased in embedding wax, and slices measuring 3 micrometers in thickness were obtained. Hematoxylin and eosin (H&E) staining was used to assess lung tissue samples.

Inflammation was evaluated using a quantification tool consisting of five distinct levels (37), which ranged from 0 to 4 to indicate the absence (0), mild (1), moderate (2), marked (3), or severe (4) condition. Edema was rated as described in a recent study (38). Furthermore, the epithelial tissue was measured. This assessment facilitates a more precise evaluation of disease stages and the severity of the condition in each study group of mice.

Nanoparticle characterization

Scanning electron microscopy (SEM) was used to investigate the morphological characteristics of the mPEG-PLGA and mPEG-PLGA/Thymoquinone formulations and dynamic light scattering (DLS) to analyze their particle size and distribution. DLS determined the particle size distribution of both mPEG-PLGA and mPEG-PLGA/Thymoquinone samples. This analysis was conducted using the Malvern Zetasizer Nano ZS 90 instrument Malvern Instruments, Worcestershire, UK) under ambient thermal condition. Furthermore, the structural characteristics of NPs were investigated utilizing MIRA3 FEG-SEM, manufactured by Tescan in the Czech Republic. For DLS analysis, drug-loaded NPs were dispersed in Ultrapure water and applied to a copper-coated mesh. Following this, the specimens were air-dried (25°C) and analyzed by Malvern Zetasizer Nano ZS90 apparatus. Additionally, drug-loaded NPs were suspended in milli-Q water to assess NP morphology and deposited onto a copper-plated grid, followed by air-drying at room temperature for subsequent observation with SEM.

Encapsulation efficacy

The encapsulation efficiency (EE%) was determined via Equation (1) by quantifying free thymoquinone in the supernatant (39) using UV-visible spectrophotometry.

$$(1) \quad EE\% = \frac{\text{Initial feeded drug} - \textit{Free drug in the supernatant}}{\text{Initial feeded drug}} \times 100$$

In vitro drug release determination

The cumulative discharge percentage of thymoquinone from mPEG-PLGA/Thymoquinone nanoparticles was assessed using a dialysis membrane. To experiment, 2 milliliter of the nanoparticles was situated into a dialysis sac. The threshold was set at a weight of ten kilodaltons. The dialysis sac was then immersed in 40 milliliter of pH 7.4 PBS solution. Continuous mixing was applied at 25 and 37 °C.

2 milliliter of nanoparticle were enclosed within a dialysis sac. The setup was subjected to stirring at both temparatures with a rotational speed of 70 revolutions per minute. At defined timespan (0.5, 1, 2, 3, and 4, 24, 48, 72, 96, 168, and 192 hours), 1 milliliter of the surface buffer containing the discharged substance was extracted. The extracted solution was replenished with an equivalent quantity of fresh buffer to ensure constant volume (40, 41). Thymoquinone concentrations were determined using UV-visible spectrophotometry (λ = 254 nm), with quantification based on a validated calibration curve (R^2 = 0.9723). Using the equation

provided, the total proportion of thymoquinone released was quantified.

$$(3) \quad cumulative\ release\ rate = \frac{v_1 \times c_i + v_2 \sum c_{(i-1)}}{m} \times 100\%$$

In the equation, v1, ci, and v2 represent PBS total volume (40 ml), drug concentration in PBS, and total sample volume (1 ml), respectively. Also, "m" indicates the initial medication concentration within the nanoparticles.

Cytotoxicity examinations

The cytotoxicity assessment of Thymoquinone-loaded mPEG-PLGA was conducted using the MTT assay. After overnight incubation of L929 and RAW 264.7 macrophage cells in 96-well plates, various concentrations of nanomedicines (ranging from 0 to 12.5 µg/ml) were applied to treat cells for 2 hours, followed by lipopolysaccharide (LPS) stimulation (1 mL, 18 hours). Then the cells were incubated with MTT solution for 4 hours (5% carbon dioxide, 37 degrees Celsius). Following the harvesting of the MTT reagent, 100 µl of DMSO was added to promote cell lysis. Final reading was at 570 nm using a microplate reader (42, 43).

Asthmatic mice

Development of asthma was through administration of ovalbumin (OVA), a popular protocol for allergic asthma. To summarize, thirty-five mice were randomly separated into five groups to study the preventive impact of mPEG-PLGA/Thymoquinone on asthma. Each group had seven mice. Dexamethasone (positive control), PBS (negative control group), thymoquinone, mPEG-PLGA, and mPEG-PLGA/Thymoquinone groups were studied. During days 0, 8, and 14, all mouse cohorts, excluding the control group receiving normal saline, underwent sensitization via intraperitoneal injection of a solution OVA (1 mg) and aluminum hydroxide gel (10 mg per milliliter of saline solution). Subsequently, from days 21 to 25, distinct mouse cohorts received intraperitoneal injections of each treatment at a dosage of 10 mg/kg. Following a 0.5-hour interval, OVA exposure was maintained at a 1% concentration through aerosolization using an ultrasonic nebulizer. Necessary assessments were conducted on day 25th (36, 44, 45).

Measurement of cytokines and IgE concentration

After 24 hours of OVA exposure, the animals were anesthetized via diethyl ether inhalation. Then blood brachial plexus blood was drawn to separate serum via centrifugation at 4 degrees Celsius, 420 g for 15 minutes. Samples were stored at -80°C until measuring cytokine and OVA-specific IgE levels. To assess IgE levels, serum specimens were mixed with the OVA diluting buffer, and quantification of IgE was executed utilizing ELISA Kits following the protocols outlined by the manufacturer at 450 nm using an ELISA reader. Figure 1 illustrates the experimental protocol, outlining the key steps and procedures followed in the study.

Mice were euthanized by blood collection via cardiac puncture, ensuring a humane and ethically compliant procedure. Following euthanasia, bronchoalveolar lavage fluid (BALF) was prepared by PBS injection into the lungs (Figure 2). BALF was collected via the trachea using a proper lavage technique, ensuring sampling from both lungs, while all histological samples were taken from the right lung (46).

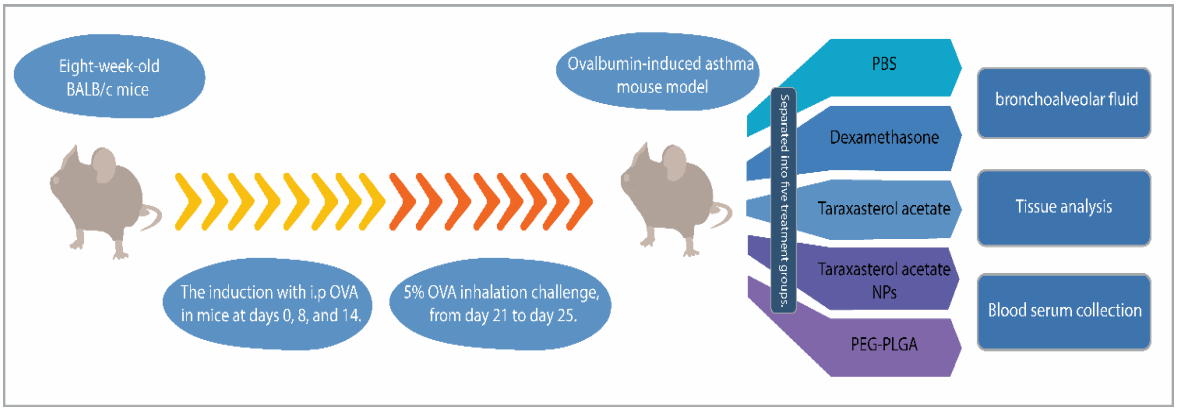

Fig. 1. Schematic representation of the experimental protocol for the OVA-induced asthma mouse model, including sensitization, inhalation challenge, treatment groups, and sample collection.

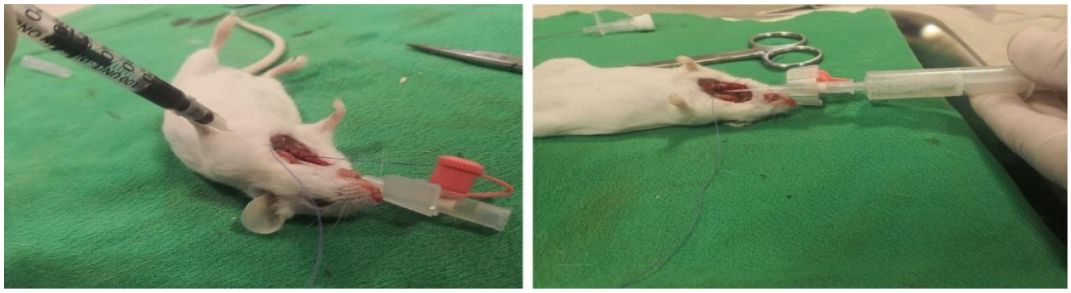

Fig. 2. Obtaining bronchoalveolar lavage fluid (BALF) by injecting PBS into the lungs

Statistical analyses

The findings were reported using appropriate descriptive parameters such as mean ± standard error of the mean (SEM). Parametric (ANOVA and Tukey-Kramer's post-hoc) and non-parametric (Kruskal-Wallis and Dunn's post-hoc) statistical tests were used for data comparison. Statistical significance was designated at $p < 0.05$. All statistical computations were executed utilizing R version 4.3.1.

RESULTS

Size Distribution and surface morphology

The morphological characteristics of the bare mPEG-PLGA (Figure 3a) and mPEG-PLGA/Thymoquinone (Figure 3b) formulations are represented. Upon loading thymoquinone, the average particle size of mPEG-PLGA increased from 201 to 255 nm. SEM analysis revealed that the mPEG-PLGA/Thymoquinone formulation exhibited a three-dimensional spherical shape with a reasonable size distribution. Notably, the smaller size appeared in SEM compared to DLS-measured hydrodynamic diameter can be attributed to the solubility of PEG in the DLS medium, which causes the structure to swell and retain a significant amount of water(47).

Encapsulation Efficiency and Entrapment Efficiency

Thymoquinone encapsulation Efficiency (EE) was determined to be 68.16% (w/w), hinting the suitability of the carrier employed in this study for thymoquinone. A PEG coating on the PLGA nanoparticles creates a protective barrier that effectively covers and shields the loaded medications. This barrier minimizes the loss of drugs during the homogenization process and helps maintain its stability, resulting in the high entrapment efficiency of thymoquinone. Effectively encapsulating significant quantities of medicines within the nanoparticles allows for sustained drug release over time(48, 49).

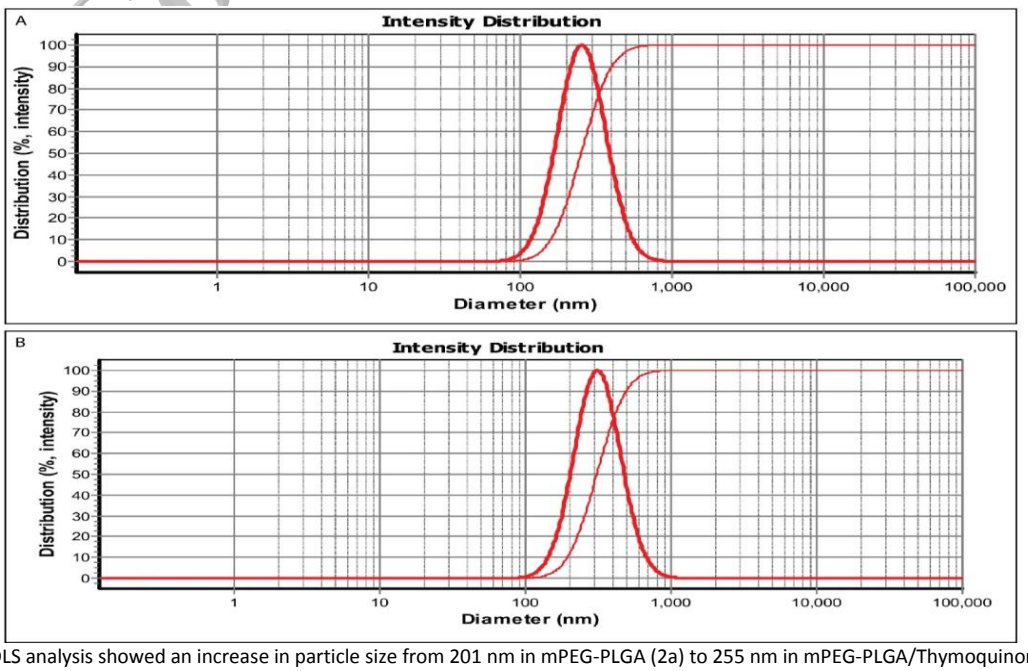

Fig. 3. DLS analysis showed an increase in particle size from 201 nm in mPEG-PLGA (2a) to 255 nm in mPEG-PLGA/Thymoquinone (2b).

In vitro thymoquinone release

Thymoquinone cumulative release from mPEG-PLGA was analyzed (Figure 4) at 37 °C, displaying an initial burst release of 51% within four hours, possibly caused by the fast dissociation of surface-attached thymoquinone. At the same time, thymoquinone at 25 °C represents a slow release, about 22%, mirroring slow-release entrapped thymoquinone. Results indicated that thymoquinone's release rate from mPEG-PLGA was higher at 37 °C compared to 25 °C; thymoquinone releases from mPEG-PLGA achieved about 80% after eight days(50). The results showed that thymoquinone released rapidly at the initial stage, after which the sustained release lasted for more than eight days.

Cell viability

Cell viability according to the MTT assay is indicated in Figure 5. The highest mPEG-PLGA/Thymoquinone concentration tested was 1000 µg/ml. Results showed that thymoquinone had an IC50 of 500 µg/ml for L929 and RAW 264.7 cells. However, thymoquinone-loaded mPEG-PLGA NPs at all concentrations up to 1000 µg/ml didn't exhibit cytotoxic effects on RAW 264.7 cells, evidenced by a cell viability rate up to 50%. This finding implied that within a particular concentration range, mPEG-PLGA/Thymoquinone exhibited high biocompatibility.

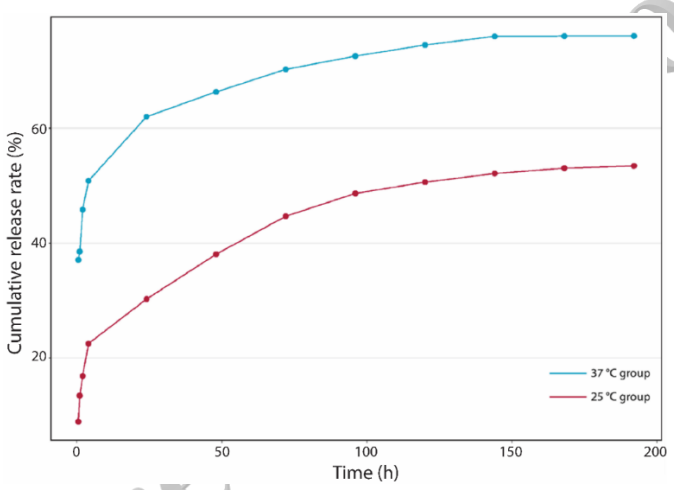

Fig. *4*. Cumulative release of thymoquinone from mPEG-PLGA at room and body temperature.

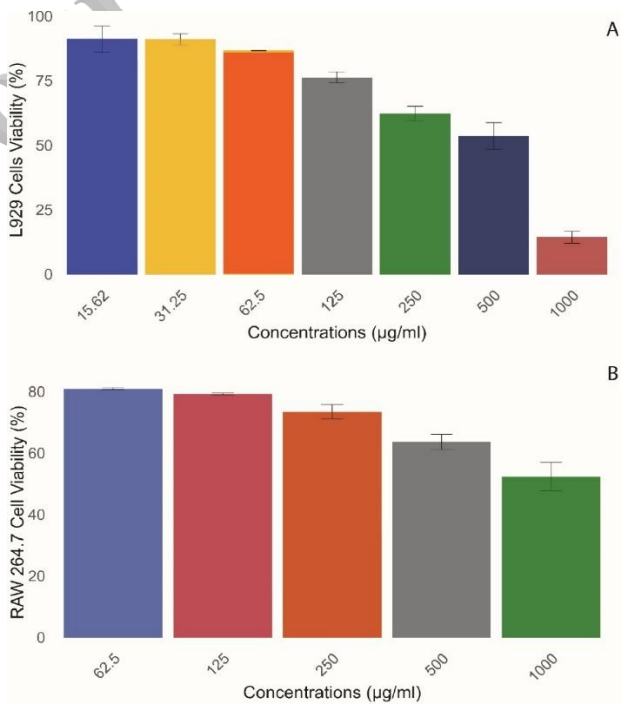

Fig. 5. Biocompatibility of mPEG-PLGA/Thymoquinone. L929 and RAW 264.7 cells were incubated with the formulation at a specified concentration range.

Changes in BALF cytokine levels and blood IgE

Levels of IL-4 and IL-13 in BALF and IgE in blood were quantified in each experimental group, as depicted in Figure 6. In response to OVA, there was a notable boost in serum IgE and BALF levels of IL-4 and IL-13. Exposure to mPEG-PLGA/Thymoquinone caused a notable fall in serum IgE and IL-4 and IL-13 concentrations in BALF, which were comparable to the dexamethasone group and considerably lower than the PBS group, upon treatment with mPEG-PLGA/Thymoquinone (Table 1). The administration of mPEG-PLGA/Thymoquinone substantially inhibited the production of these cytokines induced by OVA, indicating its potential to attenuate allergic asthma symptoms.

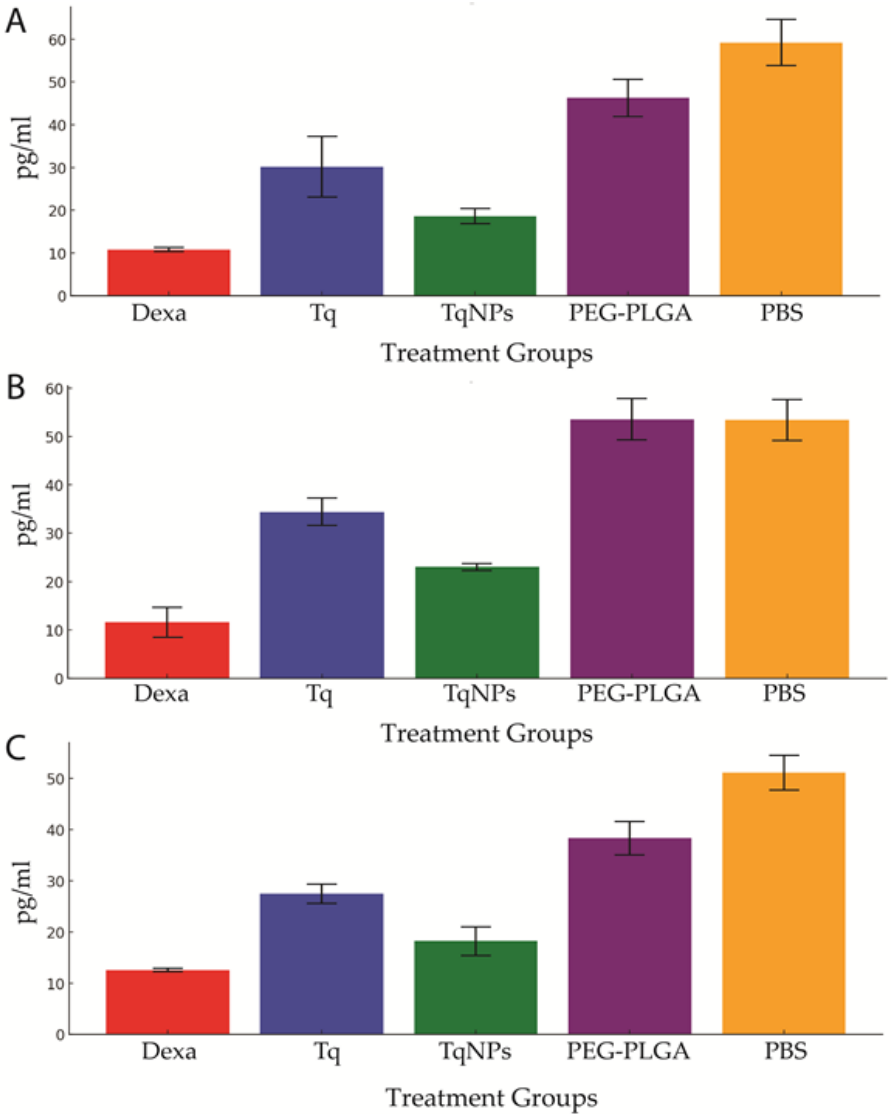

Fig. 6. Inflammatory markers in mice with OVA-induced asthma receiving mPEG-PLGA/Thymoquinone and other formulations. A) Serum IgE. B) BALF IL-13, and C) BALF IL-4. Dexa (Dexamethasone), PLGA (mPEG-PLGA), TQ (Thymoquinone), and TQ-NPs (mPEG-PLGA/Thymoquinone).

Table 1. Serum IgE and BALF ILs-13 and 4 levels in mice models of asthma. The values are mean ± SEM of (10 mice/group). * and #: P<0.05 compared to PBS and dexamethasone, respectively.

Treatments	BALF cytokine levels (pg/ml))				Serum IgE (pg/ml)	
	IL-13	P-value*	IL-4	P-value*	IgE (pg/ml)	P-value*
Dexamethasone	11.61 ± 2.976*	<0.0001	12.56 ± 0.1849*	0/0013	10.77 ± 0.3338*	0/0008
Thymoquinone	34.39 ± 2.700*	0/0031	27.50 ± 1.749*	0/031	30.18 ± 7.137*	0/0288
Thymoquinone NPs	23.06 ± 0.6028*	0/0001	18.24 ± 2.678*	0/0041	18.61 ± 1.610*	0/0030
PEG-PLGA	53.52 ± 4.13	0/094	38.38 ± 3.12	0/5321	46.25 ± 4.22	0/622
PBS	53.39 ± 4.12	-	51.12 ± 3.25	-	59.18 ± 5.22	-

* P-value from post hoc analysis compared to PBS.

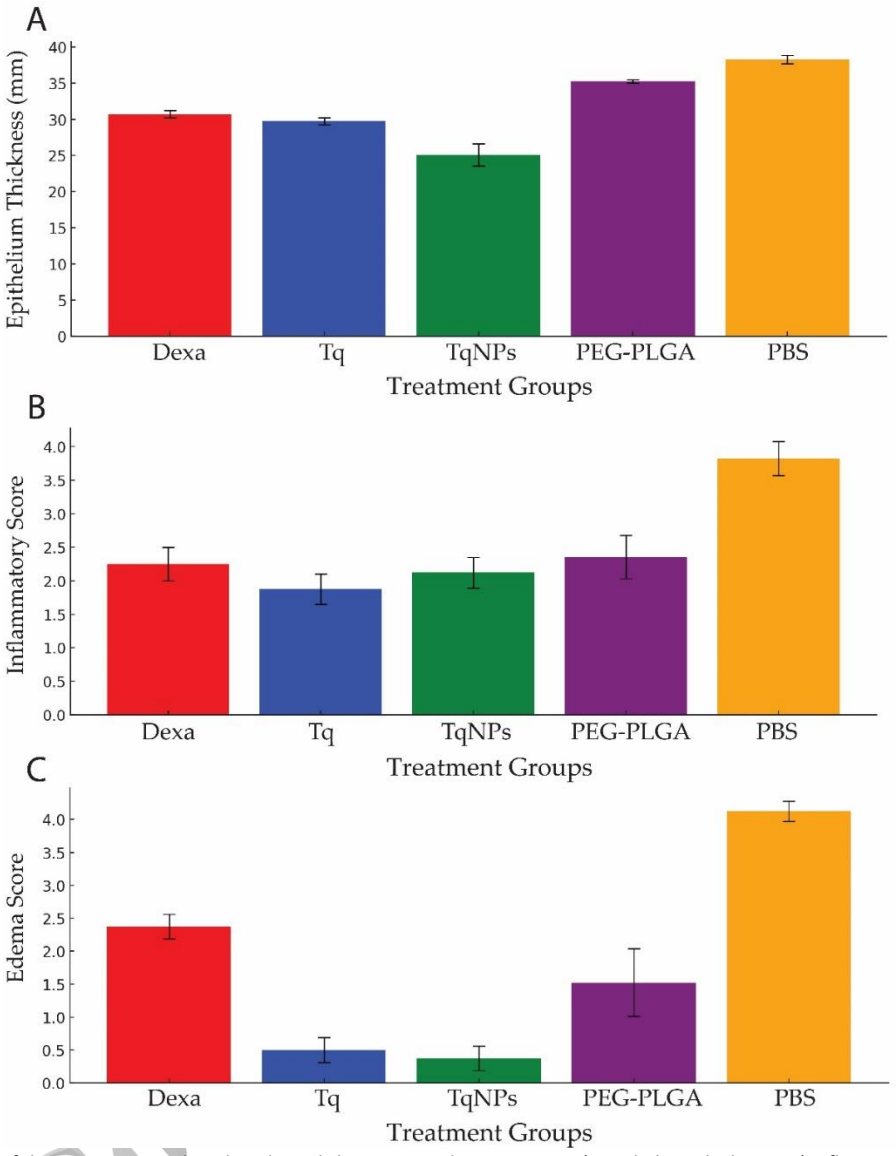

Fig. 7. Effect of thymoquinone on lung histological changes in asthmatic mice. A) Epithelium thickness. B) Inflammatory score. C) Edema score. Dexa (Dexamethasone), PEG-PLGA, Tq (Thymoquinone), and TqNPs (mPEG-PLGA/Thymoquinone). Data are expressed as mean ± SEM.

Lung histopathology assessment

Assessment of lung tissues of asthmatic mice after H&E staining revealed peribronchial inflammation, edema, and epithelial thickening in PBS-treated group (Figures 7 and 8. A), all of which were ameliorated in dexamethasone treatment group (Figures 7 and 8. B), but not toward a significant reduction in pulmonary inflammation. Comparable anti-inflammatory effects were noticed in the PEG-PLGA and Thymoquinone groups. (Table 2 and Figures 7, 8. C and 8. E), while Thymoquinone nanoparticles were superior to dexamethasone regarding the rate of inflammation reduction (Figure 7 and 8.D). Concerning perivascular edema, Thymoquinone nanoparticles and PEG-PLGA performed better than dexamethasone and PBS (Table 2 and Figure 7). In comparison with PBS-treated animals, epithelium thickness was ameliorated in all experimental groups (i.e., dexamethasone, Thymoquinone, Thymoquinone nanoparticles, and PEG-PLGA), with notably better effects being observed in mice receiving thymoquinone and thymoquinone NPs (Figure 7, Table 2).

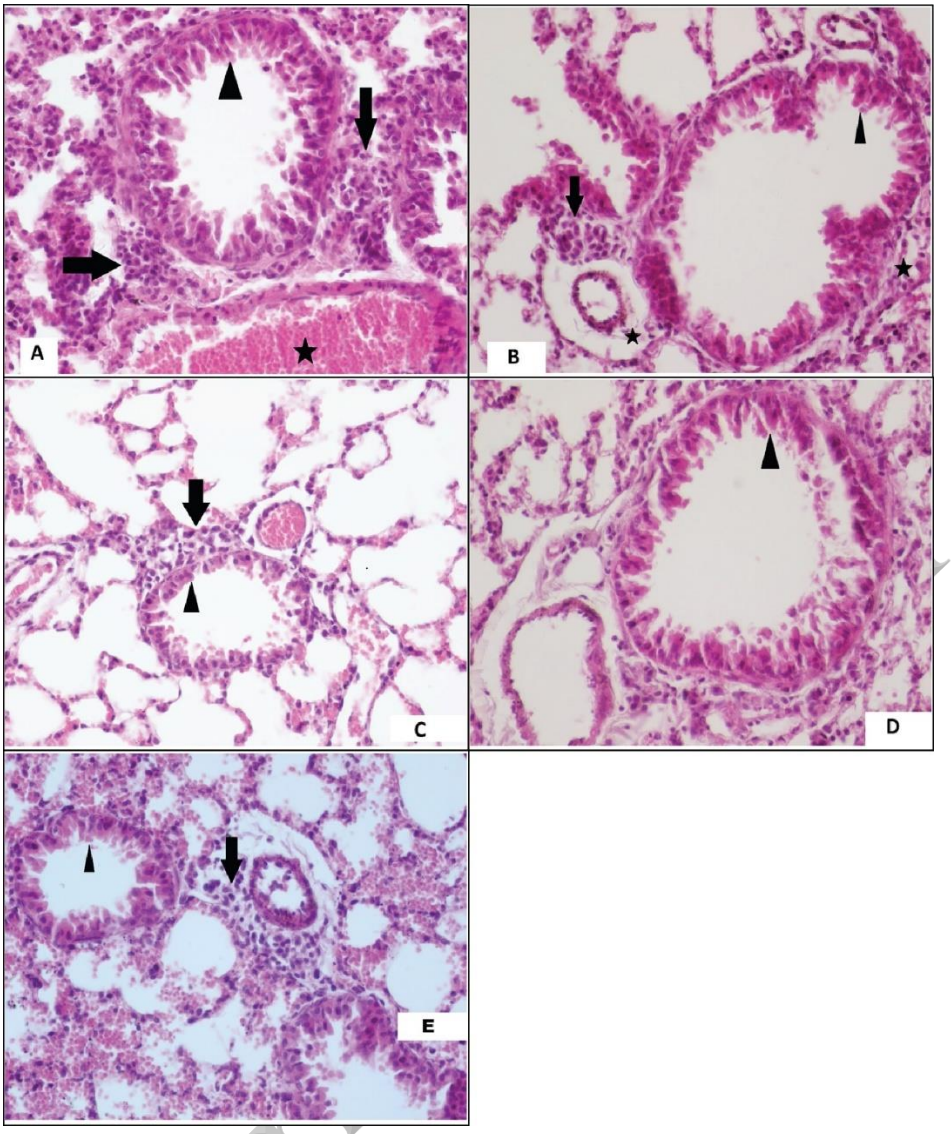

Fig. 8. Lung tissue sections, H&E staining (Groups A, B, C, D, and E represent mice treated with PBS, dexamethasone, thymoquinone, nano-Thymoquinone, and PEG-PLGA respectively). Arrow: Inflammatory cell infiltration – Arrowhead: Epithelium – Star: Edema;) (Magnification: 400×). Severe (PBS group), moderate (dexamethasone and PEG-PLGA groups), and mild (thymoquinone) perivascular and peribronchial penetration of immune cells along with edema was evident. However, nano-Thymoquinone group showed no peribronchial or perivascular infiltration of inflammatory cells or edema.

Table 2. Lung tissue inflammation scores in asthmatic mice. Data are expressed as mean ± SEM of (10 mice/group). * and #: p < 0.05 compared to control and dexamethasone groups, respectively

Experimental groups	Perivascular edema		Peribronchial inflammation		Epithelium thickness	
	Score	P-value*	Score	P-value*	Score	P-value*
Dexamethasone	2.375 ± 0.1830	0.2197	2.250 ± 0.2500	0/0033	30.67 ± 0.5184*	<0.0001
thymoquinone	0.5000 ± 0.1890*#	<0.0001	1.875± 0.2266*	0/0001	29.75 ± 0.4856*	<0.0001
Thymoquinone NPs	0.3750 ± 0.1830*#	<0.0001	2.125 ± 0.2266*	0/0011	25.09 ± 1.525*#	<0.0001
PEG-PLGA	1.524 ± 0.51*	0.4319	2.354 ± 0.325*	0/012	35.22 ± 0.25*	<0.0001
PBS	4.120 ± 0.155	-	3.824 ± 0.251	-	38.25 ± 0.574	-

* P-value from post hoc analysis compared to PBS.

DISCUSSION

Asthma is characterized by multifaceted and persistent airway inflammation (51). The main objective of ours was to establish and scrutinize the anti-inflammatory efficacy of mPEG-PLGA/Thymoquinone nanoparticles as a pioneering therapeutic intervention for managing asthma. The principal discoveries of this inquiry offer valuable insights concerning the composition characteristics, discharge kinetics, and the mode of

operation responsible for the advantageous impacts of this nanomedical solution within an ovalbumin (OVA)-induced allergic asthma model.

Thymoquinone, an active compound enriched in *Nigella sativa*, manifests robust anti-inflammatory and immunomodulatory characteristics (52). Nonetheless, its clinical utility has been constrained by intrinsic drawbacks such as substandard water solubility and bioavailability, as well as insufficient targeting of the intended site of action. Through the encapsulation of thymoquinone within mPEG-PLGA nanoparticles, this recent investigation effectively overcame these obstacles, thereby paving the path for heightened therapeutic effectiveness in asthma management. According to current information, current investigation the inaugural exploration of inhibitory impacts of Thymoquinone nanoformulations on asthma.

Within the experimental framework of OVA-induced allergic asthma, the process of OVA sensitization followed by challenge can elicit key clinical manifestations akin to asthma, notably marked by exaggerated levels of cytokines, pulmonary inflammation, and exacerbations of bronchial remodeling (53).

Traditional drug delivery approaches are hindered by various limitations, including inadequate mucosal penetration efficiency, low patient adherence to invasive administration methods, high medical expenses, suboptimal drug distribution in the body, and potential toxicity to healthy tissues (54-56). In contrast, PLGA nanoparticles offer several advantages over conventional delivery methods. These include reduced toxicity, enhanced drug availability, controlled release kinetics, and targeted delivery to lesions through diverse administration routes (57).

PLGA exhibits potential in the treatment of asthma by circumventing barriers posed by mucus and alveolar macrophages, thus enabling sustained therapeutic effects (58). PLGA nanoparticles have proven effective in specific immunotherapy for allergic asthma by shifting the Th2 response towards Th1 and mitigating allergic symptoms (59). PEG conjugation is commonly recognized as an approach showing promise to infiltrate the mucosal barrier in lungs affected by asthma and reduce endocytosis by scavenger cells and enhancing the stability of drug-loaded nanoparticles and prolongs their blood migration time (60-62).

When designing nanoparticles for asthma therapy, a critical consideration is their size. Studies indicate that nanoparticles 60-300 nm in size disperse sharply in mice tracheal mucosal layer. Moreover, surface optimization, particularly incorporating muco-inert polymers like PEG show potential in producing mucus penetrating nanoparticles, so minimizing their immune-mediated removal (63). We here synthesized mPEG-PLGA/Thymoquinone nanoparticles with a size of 255 nm, rendering them appropriate anti-asthma agents.

Furthermore, the in vitro discharge profile of the nanoparticles showed that thymoquinone released rapidly at the primary stage, after which the sustained release. This biphasic release kinetics is particularly advantageous for asthma management, as it provides an immediate therapeutic effect to alleviate acute symptoms while maintaining a consistent drug concentration in the target tissues over an extended period. Current trends in asthma management increasingly favor the use of a single inhaler for both maintenance and symptom relief. For instance, GINA guidelines recommend against using short-acting beta-agonists (SABA) alone without inhaled corticosteroids (ICS) and instead advocate for ICS/formoterol as a dual-purpose treatment for both symptom control and long-term management (64). To achieve this dual therapeutic goal, combination therapies have become a standard approach. In our study, the mPEG-PLGA/Thymoquinone formulation, with its initial burst and sustained release kinetics, shows potential for addressing both immediate and long-term asthma control using a single pharmacological product. However, while our experiments utilized intravenous administration, further studies using inhalation-based delivery methods, which are more clinically relevant for asthma patients, are necessary to confirm the favorable pharmacokinetic profile of this treatment.

We employed IL-4, IL-13, and IgE serum concentrations as biomarkers for assessing the efficacy of asthma treatment. Both thymoquinone and thymoquinone nanoparticle formulations demonstrated substantial decreases in IL-4, IL-13, and IgE levels respective to the PBS control group. IL-4 is crucial in initiating allergic responses in the airways and promoting humoral immune responses by regulating the survival and expansion of Th2 cells and IgE production. However, in the context of allergic inflammation, IL-4 does not directly regulate airway hyperresponsiveness (AHR), mucus production, or the formation of subepithelial fibrosis in vivo.

These features, characteristic of allergic asthma, are primarily influenced by IL-13, a functionally and structurally mimic of IL-4. IL-13 is considered to have a more significant part in the immune system's effector phase response in allergic asthma (65).

Additionally, several investigations have highlighted a potential link associating decreased IgE levels with improved asthma symptom management. Fahy et al. suggested that focusing on increased IgE concentrations, found in asthmatic individuals, could represent a promising strategy (66). Tanaka et al. also noted a direct correlation between increased IgE concentrations and poorly managed asthma indicating that neutralizing IgE therapeutically could optimize therapeutic efficacy (67). Moreover, while this study provides precious visions, some limitations must be appreciated. One limitation is the exclusive use of female mice, which may not capture the biological variations that could occur in male subjects. A suggestion for further research is to run the same experiments in male mice, offering a more all-embracing understanding of the therapeutic effects and potential sex-based differences in a preclinical setting. Additionally, factors such as genetic background, environmental influences, and sample size should be considered in future studies to ensure robust and widely applicable findings. Addressing these limitations would strengthen the reliability of the results and contribute to a more nuanced understanding of the research question.

CONCLUSION

We successfully prepared mPEG-PLGA/Thymoquinone nanoparticles in this study. The formulation achieved an optimal encapsulation efficiency and exhibited a particle size of approximately 255 nm on average. Drug release testing in vitro showed that mPEG-PLGA/Thymoquinone demonstrated sustained release behavior following an initial burst release. Moreover, compared to the group treated with thymoquinone alone, administration of mPEG-PLGA/Thymoquinone to asthmatic rodents supressed Pro-inflammatory cells, Th2 cytokines, and OVA-specific IgE levels. We conclude that mPEG-PLGA can be employed as an encouraging delivery platform to improve the effectiveness of thymoquinone in asthma treatment. Importantly, these results provide novel evidence for the anti-inflammatory activity of mPEG-PLGA/Thymoquinone in the context of OVA-induced allergic asthma.

CONFLICT OF INTEREST

There is no conflict of interest.

ACKNOWLEDGEMENTS

We would like to sincerely acknowledge and express our gratitude for the financial support provided by the North Khorasan University of Medical Sciences, (Code number: 980017, and Ethic approval code number: IR.NKUMS.REC.1399.077).

AUTHOR CONTRIBUTIONS

M. R. and S.Gh. Wrote the original draft, Methodology, Formal analysis, M. V. did animal experiments. A.H., Designing and conceptualization, project administration F. O., supervision, writing, reviewing and editing.

REFERENCES

1. Humbert M. Asthma, a priority for the allergist. Allergy. 2006;61(5):515-517.
2. Nunes C, Pereira AM, Morais-Almeida M. Asthma costs and social impact. Asthma Res Pract. 2017;3:1-11.
3. Xu M, Dong C. IL-25 in allergic inflammation. Immunol Rev. 2017;278(1):185-191.
4. Kudo M, Ishigatsubo Y, Aoki I. Pathology of asthma. Front Microbiol. 2013;4:263.
5. Koch S, Sopel N, Finotto S, Finotto S. Th9 and other IL-9-producing cells in allergic asthma. Semin Immunopathol; 2017: 39 (1): 55-68.Springer.
6. Verma M, Liu S, Michalec L, Sripada A, Gorska MM, Alam R. Experimental asthma persists in IL-33 receptor knockout mice because of the emergence of thymic stromal lymphopoietin–driven IL-9+ and IL-13+ type 2 innate lymphoid cell subpopulations. J Allergy Clin Immunol. 2018;142(3):793-803.
7. Borak J, Lefkowitz R. Bronchial hyperresponsiveness. Occup Med. 2016;66(2):95-105.
8. Boulet L-P. Airway remodeling in asthma: update on mechanisms and therapeutic approaches. Curr Opin Pulm Med. 2018;24(1):56-62.
9. Papi A, Blasi F, Canonica GW, Morandi L, Richeldi L, Rossi A. Treatment strategies for asthma: reshaping the concept of asthma management. Allergy Asthma Clin Immunol. 2020;16:1-11.
10. Reddel HK, Bacharier LB, Bateman ED, Brightling CE, Brusselle GG, Buhl R, et al. Global Initiative for Asthma Strategy 2021: executive summary and rationale for key changes. Am J Respir Crit Care Med. 2022;205(1):17-35.
11. Katsaounou P, Buhl R, Brusselle G, Pfister P, Martínez R, Wahn U, et al. Omalizumab as alternative to chronic use of oral corticosteroids in severe asthma. Respir Med. 2019;150:51-62.
12. Bårnes CB, Ulrik CS. Asthma and adherence to inhaled corticosteroids: current status and future perspectives. Respir Care. 2015;60(3):455-468.

13. Volmer T, Effenberger T, Trautner C, Buhl R. Consequences of long-term oral corticosteroid therapy and its side-effects in severe asthma in adults: a focused review of the impact data in the literature. Eur Respir J. 2018;52(4).
14. Berger M. Adverse effects of IgG therapy. J Allergy Clin Immunol Pract. 2013;1(6):558-566.
15. Cherin P, Marie I, Michallet M, Pelus E, Dantal J, Crave J-C, et al. Management of adverse events in the treatment of patients with immunoglobulin therapy: a review of evidence. Autoimmun Rev. 2016;15(1):71-81.
16. Moghaddam FA, Ebrahimian M, Oroojalian F, Yazdian-Robati R, Kalalinia F, Tayebi L, et al. Effect of thymoquinone-loaded lipid–polymer nanoparticles as an oral delivery system on anticancer efficiency of doxorubicin. J Nanostruct Chem. 2022:1-12.
17. Amaral-Machado L, Oliveira WN, Moreira-Oliveira SS, Pereira DT, Alencar EN, Tsapis N, et al. Use of natural products in asthma treatment. Evid Based Complement Alternat Med. 2020;2020(1):1021258.
18. Kan S, Hariyadi DM, Grainge C, Knight DA, Bartlett NW, Liang M. Airway epithelial-targeted nanoparticles for asthma therapy. Am J Physiol Lung Cell Mol Physiol. 2020;318(3):L500-L509.
19. Omidi M, Malakoutian M, Choolaei M, Oroojalian F, Haghiralsadat F, Yazdian F. A Label-Free detection of biomolecules using micromechanical biosensors. Chin Phys Lett. 2013;30(6):068701.
20. Hassanpour S, Behnam B, Baradaran B, Hashemzaei M, Oroojalian F, Mokhtarzadeh A, et al. Carbon based nanomaterials for the detection of narrow therapeutic index pharmaceuticals. Talanta. 2021;221:121610.
21. Feyziazar M, Amini M, Jahanban-Esfahlan A, Baradaran B, Oroojalian F, Kamrani A, et al. Recent advances on the piezoelectric, electrochemical, and optical biosensors for the detection of protozoan pathogens. TrAC Trends Anal Chem. 2022;157:116803.
22. Bidar N, Oroojalian F, Baradaran B, Eyvazi S, Amini M, Jebelli A, et al. Monitoring of microRNA using molecular beacons approaches: Recent advances. TrAC Trends Anal Chem. 2020;131:116021.
23. Andisheh F, Oroojalian F, Shakour N, Ramezani M, Shamsara J, Khodaverdi E, et al. Docetaxel encapsulation in nanoscale assembly micelles of folate-PEG-docetaxel conjugates for targeted fighting against metastatic breast cancer in vitro and in vivo. Int J Pharm. 2021;605:120822.
24. Beygi M, Oroojalian F, Azizi-Arani S, Hosseini SS, Mokhtarzadeh A, Kesharwani P, et al. Multifunctional nanotheranostics for overcoming the blood–brain barrier. Adv Funct Mater. 2024;34(19):2310881.
25. Rahmanian M, Ghahremani A, Kesharwani P, Oroojalian F, Sahebkar A. Nanomedicine innovations in spinal cord injury management: Bridging the gap. Environ Res. 2023;235:116563.
26. Pishavar E, Oroojalian F, Salmasi Z, Hashemi E, Hashemi M. Recent advances of dendrimer in targeted delivery of drugs and genes to stem cells as cellular vehicles. Biotechnol Prog. 2021;37(4):e3174.
27. Cao H, Liu L, Wang J, Gong M, Yuan R, Lu J, et al. Effects of rAmb a 1-loaded PLGA-PEG nanoparticles in a murine model of allergic conjunctivitis. Molecules. 2022;27(3):598.
28. Beygi M, Oroojalian F, Hosseini SS, Mokhtarzadeh A, Kesharwani P, Sahebkar A. Recent progress in functionalized and targeted polymersomes and chimeric polymeric nanotheranostic platforms for cancer therapy. Prog Mater Sci. 2023;140:101209.
29. Vij N. Synthesis and evaluation of airway-targeted PLGA-PEG nanoparticles for drug delivery in obstructive lung diseases. Nanoparticles in Biology and Medicine: Methods and Protocols: Springer. 2020;147-154.
30. Darakhshan S, Pour AB, Colagar AH, Sisakhtnezhad S. Thymoquinone and its therapeutic potentials. Pharmacol Res. 2015;95:138-158.
31. Fatima Shad K, Soubra W, Cordato DJ. The role of thymoquinone, a major constituent of Nigella sativa, in the treatment of inflammatory and infectious diseases. Clin Exp Pharmacol Physiol. 2021;48(11):1445-1453.
32. El Mezayen R, El Gazzar M, Nicolls MR, Marecki JC, Dreskin SC, Nomiyama H. Effect of thymoquinone on cyclooxygenase expression and prostaglandin production in a mouse model of allergic airway inflammation. Immunol lett. 2006;106(1):72-81.
33. Kohandel Z, Farkhondeh T, Aschner M, Samarghandian S. Anti-inflammatory effects of thymoquinone and its protective effects against several diseases. Biomed Pharmacother. 2021;138:111492.
34. El Gazzar M, El Mezayen R, Nicolls MR, Marecki JC, Dreskin SC. Downregulation of leukotriene biosynthesis by thymoquinone attenuates airway inflammation in a mouse model of allergic asthma. Biochim Biophys Acta Gen Subj. 2006;1760(7):1088-1095.
35. Shaterzadeh-Yazdi H, Noorbakhsh M-F, Hayati F, Samarghandian S, Farkhondeh T. Immunomodulatory and anti-inflammatory effects of thymoquinone. Cardiovasc Haematol Disord Drug Targets. 2018;18(1):52-60.
36. Ghazanfary S, Rahmanian M, Vatanchian M, Haghbin A, Shakeri F, Oroojalian F. Characterization and Efficacy Evaluation of mPEG-PLGA/Taraxasterol Acetate Nanoparticles as Nano-Therapeutic Agents in Asthma Management. BioNanoScience. 2025;15(1):124.
37. Cao R, Dong X-W, Jiang J-X, Yan X-F, He J-S, Deng Y-M, et al. M3 muscarinic receptor antagonist bencycloquidium bromide attenuates allergic airway inflammation, hyperresponsiveness and remodeling in mice. Eur J Pharmacol. 2011;655(1-3):83-90.
38. Venturini CL, Macho A, Arunachalam K, de Almeida DAT, Rosa SIG, Pavan E, et al. Vitexin inhibits inflammation in murine ovalbumin-induced allergic asthma. Biomed Pharmacother. 2018;97:143-151.

39. Massella D, Celasco E, Salaün F, Ferri A, Barresi AA. Overcoming the limits of flash nanoprecipitation: Effective loading of hydrophilic drug into polymeric nanoparticles with controlled structure. Polymers. 2018;10(10):1092.
40. Ebrahimian M, Mahvelati F, Malaekeh-Nikouei B, Hashemi E, Oroojalian F, Hashemi M. Bromelain loaded lipid-polymer hybrid nanoparticles for oral delivery: Formulation and characterization. Appl Biochem Biotechnol. 2022;194(8):3733-3748.
41. Ebrahimpour M, Akhlaghi M, Hemati M, Ghazanfary S, Shahriary S, Ghalekohneh SJ, et al. In vitro evaluation and comparison of anticancer, antimicrobial, and antifungal properties of thyme niosomes containing essential oil. Nanomed J. 2022;9(4).
42. El-Hammadi MM, Small-Howard AL, Jansen C, Fernández-Arévalo M, Turner H, Martín-Banderas L. Potential use for chronic pain: Poly (Ethylene Glycol)-Poly (Lactic-Co-Glycolic Acid) nanoparticles enhance the effects of Cannabis-Based terpenes on calcium influx in TRPV1-Expressing cells. Int J Pharm. 2022;616:121524.
43. Pishavar E, Oroojalian F, Ramezani M, Hashemi M. Cholesterol-conjugated PEGylated PAMAM as an efficient nanocarrier for plasmid encoding interleukin-12 immunogene delivery toward colon cancer cells. Biotechnol Prog. 2020;36(3):e2952.
44. Wang W, Zhu R, Xie Q, Li A, Xiao Y, Li K, et al. Enhanced bioavailability and efficiency of curcumin for the treatment of asthma by its formulation in solid lipid nanoparticles. Int J Nanomed. 2012:3667-3677.
45. Yao Y, Zeng Q-X, Deng X-Q, Tang G-N, Guo J-B, Sun Y-Q, et al. Connexin 43 upregulation in mouse lungs during ovalbumin-induced asthma. PLoS One. 2015;10(12):e0144106.
46. Van Hoecke L, Job ER, Saelens X, Roose K. Bronchoalveolar Lavage of Murine Lungs to Analyze Inflammatory Cell Infiltration. Journal of visualized experiments : JoVE. 2017(123).
47. Jusu S, Obayemi J, Salifu A, Nwazojie C, Uzonwanne V, Odusanya O, et al. Drug-encapsulated blend of PLGA-PEG microspheres: in vitro and in vivo study of the effects of localized/targeted drug delivery on the treatment of triple-negative breast cancer. Sci Rep. 2020;10(1):14188.
48. Ullah S, Shah MR, Shoaib M, Imran M, Elhissi AM, Ahmad F, et al. Development of a biocompatible creatinine-based niosomal delivery system for enhanced oral bioavailability of clarithromycin. Drug Deliv. 2016;23(9):3480-3491.
49. Fahmy SA, Mahdy NK, Al Mulla H, ElMeshad AN, Issa MY, Azzazy HME-S. PLGA/PEG nanoparticles loaded with cyclodextrin-Peganum harmala alkaloid complex and ascorbic acid with promising antimicrobial activities. Pharmaceutics. 2022;14(1):142.
50. Noor NS, Kaus NHM, Szewczuk MR, Hamid SBS. Formulation, Characterization and Cytotoxicity Effects of Novel Thymoquinone-PLGA-PF68 Nanoparticles. Int J Mol Sci. 2021;22(17).
51. Sockrider M, Fussner L. What Is Asthma? Am J Respir Crit Care Med. 2020;202(9):P25-p26.
52. Majdalawieh AF, Fayyad MW. Immunomodulatory and anti-inflammatory action of Nigella sativa and thymoquinone: A comprehensive review. Int Immunopharmacol. 2015;28(1):295-304.
53. Nials AT, Uddin S. Mouse models of allergic asthma: acute and chronic allergen challenge. Disease Models & Mechanisms. 2008;1(4-5):213-220.
54. Swider E, Koshkina O, Tel J, Cruz LJ, de Vries IJM, Srinivas M. Customizing poly(lactic-co-glycolic acid) particles for biomedical applications. Acta Biomaterialia. 2018;73:38-51.
55. Essa D, Kondiah PPD, Choonara YE, Pillay V. The Design of Poly(lactide-co-glycolide) Nanocarriers for Medical Applications. Front Bioeng Biotechnol. 2020;8:48.
56. El-Hammadi MM, Arias JL. Recent Advances in the Surface Functionalization of PLGA-Based Nanomedicines. Nanomaterials (Basel, Switzerland). 2022;12(3).
57. Guo X, Zuo X, Zhou Z, Gu Y, Zheng H, Wang X, et al. PLGA-Based Micro/Nanoparticles: An Overview of Their Applications in Respiratory Diseases. Int J Mol Sci. 2023;24(5).
58. Li J, Zheng H, Xu E-Y, Moehwald M, Chen L, Zhang X, et al. Inhalable PLGA microspheres: Tunable lung retention and systemic exposure via polyethylene glycol modification. Acta Biomaterialia. 2021;123:325-334.
59. Xiao X, Zeng X, Zhang X, Ma L, Liu X, Yu H, et al. Effects of Caryota mitis profilin-loaded PLGA nanoparticles in a murine model of allergic asthma. Int J Nanomed. 2013:4553-4562.
60. Vllasaliu D, Fowler R, Stolnik S. PEGylated nanomedicines: recent progress and remaining concerns. Expert Opin Drug Deliv. 2014;11(1):139-154.
61. Owens DE, 3rd, Peppas NA. Opsonization, biodistribution, and pharmacokinetics of polymeric nanoparticles. Int J Pharm. 2006;307(1):93-102.
62. Perry JL, Reuter KG, Kai MP, Herlihy KP, Jones SW, Luft JC, et al. PEGylated PRINT nanoparticles: the impact of PEG density on protein binding, macrophage association, biodistribution, and pharmacokinetics. Nano lett. 2012;12(10):5304-5310.
63. Schneider CS, Xu Q, Boylan NJ, Chisholm J, Tang BC, Schuster BS, et al. Nanoparticles that do not adhere to mucus provide uniform and long-lasting drug delivery to airways following inhalation. Sci Adv. 2017;3(4):e1601556.
64. Levy ML, Bacharier LB, Bateman E, Boulet L-P, Brightling C, Buhl R, et al. Key recommendations for primary care from the 2022 Global Initiative for Asthma (GINA) update. NPJ Prim Care Respir Med. 2023;33(1):1-13.
65. Gour N, Wills-Karp M. IL-4 and IL-13 signaling in allergic airway disease. Cytokine. 2015;75(1):68-78.
66. Fahy JV. Reducing IgE levels as a strategy for the treatment of asthma. Clin Exp Allergy : journal of the

British Society for Allergy and Clinical Immunology. 2000;30 Suppl 1:16-21.
67. Tanaka A, Jinno M, Hirai K, Miyata Y, Mizuma H, Yamaguchi M, et al. Longitudinal increase in total IgE levels in patients with adult asthma: an association with poor asthma control. Respir Med. 2014;15(1):144.